Biomedicine & Pharmacotherapy 183 (2025) 117856

Contents lists available at ScienceDirect

Biomedicine & Pharmacotherapy

journal homepage: www.elsevier.com/locate/biopha

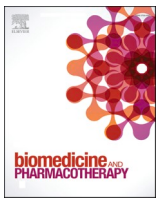

SMEPPI: An indenone derivative that selectively inhibits M1 macrophage activation and enhances phagocytic activity

Ji Hyun Oh [a], Mi Gyeong Jeong [a], Soheun Lee [a], Jihae Lim [a], Jio Kang [a], Myung Ae Bae [c], Jin-Hee Ahn [d], Jeong-Ho Hong [e], Eun Sook Hwang [a,b,*]

[a] College of Pharmacy and Graduate School of Pharmaceutical Sciences, Ewha Womans University, Seoul 03760, South Korea
[b] Gradutate Program in Innovative Biomaterials Convergence, Ewha Womans University, Seoul 03760, South Korea
[c] Drug Discovery Platform Research Center, Korea Research Institute of Chemical Technology (KRICT), Daejeon 34114, South Korea
[d] Department of Chemistry, Gwangju Institute of Science and Technology, Gwangju 61005, South Korea
[e] Division of Life Sciences, Korea University, Seoul 02841, South Korea

ARTICLE INFO

Keywords:
Acute lung injury
Macrophage
Mortality
Phagocytosis
P65
SMEPPI

ABSTRACT

SMEPPI is a small molecule synthesized as a derivative of KR-62980 that has anti-diabetic and anti-inflammatory activities. Despite the established physiological effects of KR-62980, the effects and benefits of SMEPPI remain largely unexplored. This study investigated the immunomodulatory functions of SMEPPI on macrophages and inflammatory diseases. SMEPPI did not affect the differentiation and maturation of bone marrow-derived monocytes into macrophages, nor did it affect the proliferation of M1 or M2 macrophages. Although SMEPPI did not affect M2 macrophage polarization, it significantly inhibited IL-1β and IL-6 cytokine production in both M1 macrophages and activated RAW264.7 macrophages. Importantly, SMEPPI inhibited the expression and phosphorylation of NF-κB p65 through inhibition of Akt expression, preventing its translocation to the nucleus. It also promoted p65 degradation through the stimulation of the proteasomal degradation pathway by inducing the expression of proteasome-related genes, thereby inhibiting p65 transcriptional activity. SMEPPI also enhanced the expression of various molecules associated with macrophage phagocytosis, including CD68, CD33, and lectins, thereby increasing phagocytic activity. Moreover, SMEPPI mitigated lipopolysaccharides-induced acute lung injury by suppressing IL-1β and IL-6 production in M1 macrophages and reduced mortality related to severe lung injury. These findings indicate that SMEPPI effectively regulates inflammatory diseases by impeding p65-induced cytokine production and enhancement of phagocytosis by M1 macrophages.

1. Introduction

Inflammation is a highly regulated process in response to microbial infections or tissue injury, involving a balance of pro- and anti-inflammatory components that rapidly resolve harmful conditions and restore homeostasis [1,2]. In the early stages of inflammation, macrophages recognize and eliminate foreign antigens via phagocytosis while simultaneously presenting antigenic peptides to T lymphocytes, thereby resulting in activation of an acquired immune response involving the production of antibodies, cytokines, and memory cells [3]. Macrophage activity transitions from a pro-inflammatory to an anti-inflammatory response, contributing to homeostasis by the elimination of harmful entities [4]. Macrophages play a crucial role in the innate immune response and regulate innate and adaptive immune responses as a result of their polarization and differentiation into distinct phenotypes. When exposed to lipopolysaccharides (LPS) and interferons, resting macrophages polarize into pro-inflammatory M1 macrophages (classically activated). In contrast, interleukin (IL)-4 and IL-13 promote the development of anti-inflammatory M2 macrophages (alternatively activated) [5]. M1 and M2 macrophages are central to host defense mechanisms and responses to tissue remodeling, respectively, and they express specific surface biomarkers and secrete distinct cytokines. M1 markers include CD80 and IL-6, while M2 markers comprise arginase-1 (Arg-1) and IL-10. While the balance between M1 and M2 macrophages is essential for maintaining normal physiological homeostasis, their aberrant hyperactivation and imbalance can lead to deleterious effects, causing lesions and contributing to various inflammatory diseases, including arthritis, lung injury, and sepsis [6].

* Correspondence to: Ewha Womans University, C206 Science Building, 52 Ewhayeodae-Gil, Seodaemun-Gu, Seoul 03760, South Korea.
E-mail address: eshwang@ewha.ac.kr (E.S. Hwang).

https://doi.org/10.1016/j.biopha.2025.117856
Received 18 November 2024; Received in revised form 3 January 2025; Accepted 13 January 2025

Macrophages differentiate from myeloid progenitor cells derived from hematopoietic stem cells in the bone marrow (BM) [7]. Upon stimulation with macrophage colony-stimulating factor (M-CSF), myeloid progenitor cells proliferate and develop into monocytes, which then enter the bloodstream and migrate to various tissues. Depending on the local cytokines, growth factors, and the presence of pathogens or cellular debris, monocytes differentiate into macrophages, adapting to their microenvironments and exhibiting tissue-specific functions [8]. Tissue-resident macrophages, including Kupffer cells in the liver, alveolar macrophages in the lungs, microglial in the central nervous system, and osteoclasts in the bone, reside permanently in specific tissues [3]. Circulating monocytes migrate to damaged or infected tissues, where they transform into macrophages, which then mediate the immune response and facilitate tissue repair [9]. Given their multiple roles in immunity, inflammation, and tissue homeostasis, macrophages represent promising therapeutic targets for treating various diseases [10]. Thus, the identification and characterization of small molecules that can modulate macrophage activation and phagocytosis are highly promising avenues for tacking macrophage-mediated inflammatory diseases.

Indenone derivatives have been developed as peroxisome proliferator-activated receptor γ (PPARγ) agonists and have been shown to exhibit extensive anti-oxidative, anti-hyperglycemic, anti-dyslipidemic, anti-tumor, and anti-inflammatory properties [11–16]. Among these, KR-62980 [1-(transmethylimino-N-oxy)-6-(2-morpholinoethoxy)-3-phenyl-1H-indene-2-carboxylic acid ethyl ester] is a derivative with a modified indenone structure that inhibits fat accumulation through activation of PPARγ suppressor, thus highlighting its potential as a therapeutic agent with anti-diabetic and reduced adipogenic effects [17–19]. Additionally, KR-62980 exerts anti-allergic effects and alleviates allergen-induced airway inflammation, further supporting its role as an anti-inflammatory agent [20]. SMEPPI [6-(2-(1,1-dioxidothiomorpholino) ethoxy)-3-(2,4-difluorophenyl)-2-(6-methoxypyridin-3-yl)-1*H*-inden-1-one], a newly synthesized derivative of KR-62980, retains the core indenone structure while incorporating functional modifications, such as thiomorpholinoethoxy, difluorophenyl, and methoxypyridinyl groups, which may lead to additional biological effects.

In this study, we investigated the effects of the indene derivative SMEPPI on macrophage activation and polarization and explored its anti-inflammatory effects *in vivo*.

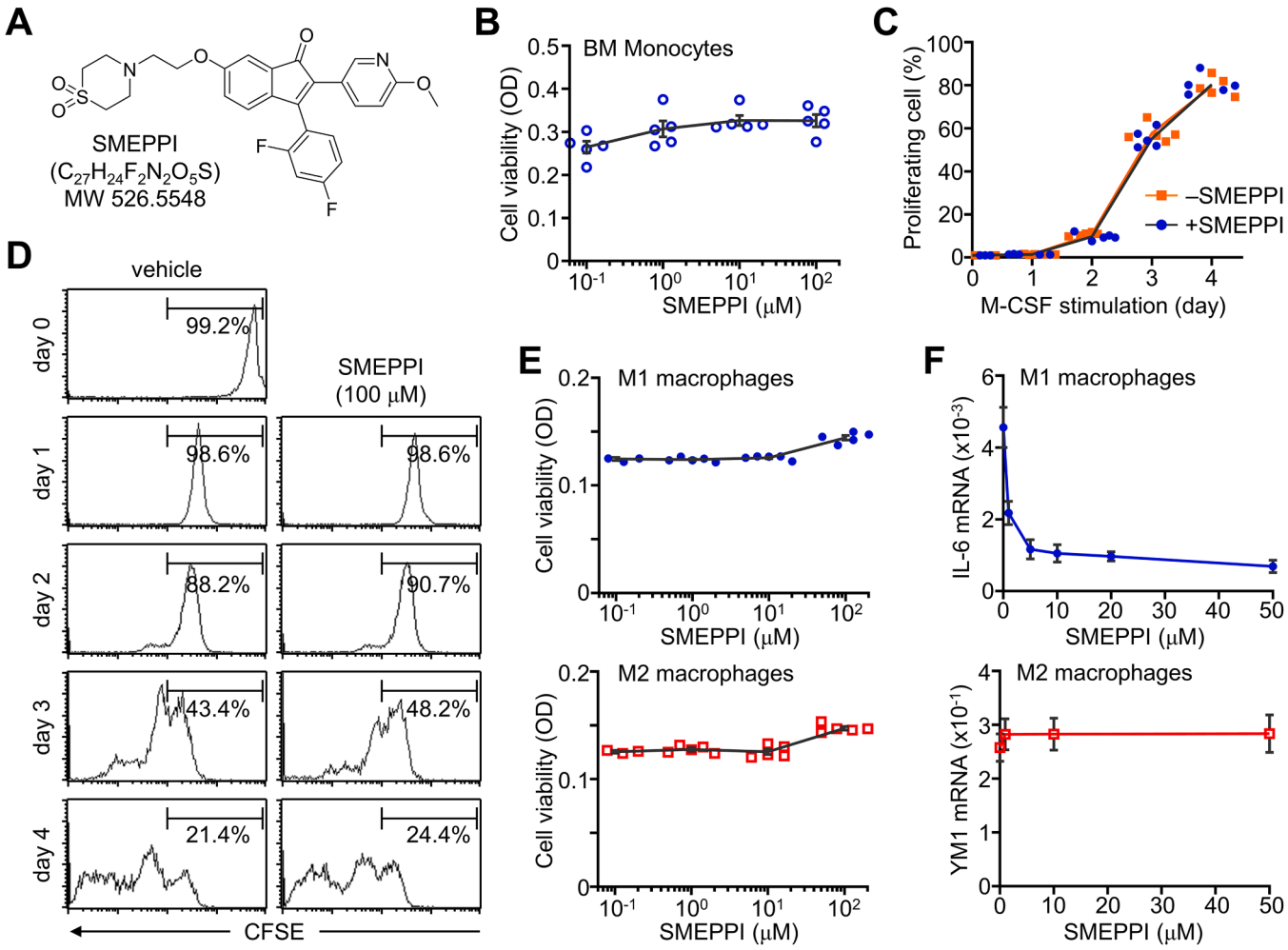

Fig. 1. Effects of SMEPPI on the proliferation and polarization of BMDMs. (**A**) Structure of SMEPPI. (**B–D**) BMDMs were isolated and cultured in the presence of M-CSF. The effects of various concentrations of SMEPPI on BMDM cell viability were analyzed (**B**). Cell proliferation of BMDMs was assayed in the presence or absence of SMEPPI for 4 days (**C**). Flow cytometric analysis of BMDM proliferation after treatment with SMEPPI was conducted (**D**). (**E, F**) Macrophage polarization into M1 and M2 was induced in the presence of SMEPPI. Cell viability was assessed for the M1 and M2 macrophages (**E**), and biomarkers of M1 and M2 macrophages were quantitatively analyzed (**F**). The data represent the mean ± SEM of five independent experiments.

2. Results

2.1. Effects of SMEPPI on macrophage differentiation and polarization

To examine the effects of the indenone derivative SMEPPI on macrophage differentiation and maturation, BM-derived monocytes (BMDMs) were treated with various concentrations of SMEPPI (Fig. 1A). SMEPPI did not exhibit cytotoxicity toward monocytes, nor did it affect cell proliferation in response to M-CSF treatment during differentiation into macrophages (Fig. 1B and C). Furthermore, SMEPPI had no effect on the cell cycle progression of macrophages over a period of 4 days following M-CSF stimulation (Fig. 1D). Similarly, SMEPPI did not affect the viability of M1- or M2- polarized macrophages (Fig. 1E). However, SMEPPI dose-dependently decreased the expression of IL-6, a signature marker of M1 macrophages, and rapidly reduced its level by more than 50 % at a concentration of 1 μM. In contrast, the expression of Ym1, a representative marker of M2 macrophages, was not affected by SMEPPI (Fig. 1F). These findings suggest that SMEPPI regulates the activity of polarized M1 macrophages without affecting macrophage differentiation or proliferation.

2.2. Suppression of M1-driven inflammatory cytokines by SMEPPI

To verify the regulatory effect of SMEPPI on the activities of polarized M1 and M2 macrophages, we treated M1 and M2 macrophages with SMEPPI at concentrations of 10 μM or less during the polarization process and then analyzed the expression of cytokines. SMEPPI significantly and concentration-dependently reduced IL-1β and IL-6 expression in BM-derived M1 macrophages (Fig. 2A). These results were also confirmed using unstimulated and LPS-stimulated RAW264.7 macrophages. SMEPPI significantly decreased the expression of IL-1β, IL-6, and TNF-α at both basal and LPS-stimulated levels in RAW264.7 cells (Fig. 2B). In contrast, the expression of ARG1, an M2-specific marker, was not altered by SMEPPI in IL-4 and IL-13-treated RAW264.7 cells (Fig. 2C). Therefore, SMEPPI appears to selectively inhibit inflammatory cytokine production in M1 macrophages without affecting M2 macrophages.

2.3. Inhibition of NF-κB p65 expression and activation by SMEPPI

To understand the molecular mechanisms underlying the inhibition of M1-driven inflammatory cytokines by SMEPPI, we examined the expression levels of NF-κB signaling molecules involved in the production of IL-1β, IL-6, and TNF-α. Interestingly, both the expression and phosphorylation levels of NF-κB p65 (p65) were affected by SMEPPI treatment. The phosphorylation of p65 was decreased in a dose-dependent manner by treatment with SMEPI, and p65 expression was markedly decreased at a concentration of 10 μM. In contrast, IκB

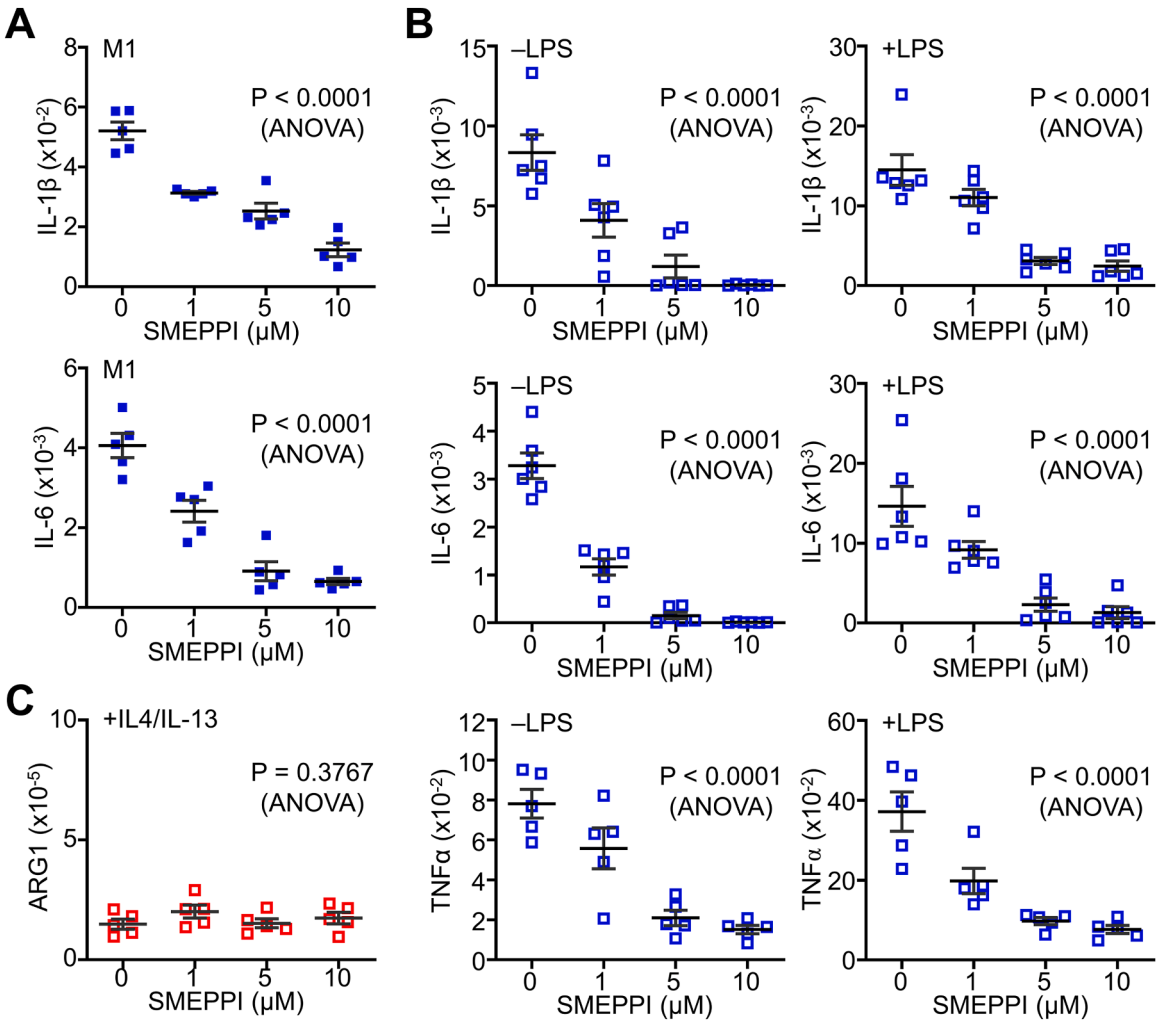

Fig. 2. Inhibitory activity of SMEPPI on M1 macrophages. (**A**) Inhibitory effect of SMEPPI on IL-1β and IL-6 production by primary M1 macrophages. (**B**) Inhibition of IL-1β, IL-6, and TNF-α by SMEPPI in RAW264.7 macrophages with or without LPS stimulation. (**C**) No significant effect of SMEPPI on the expression of M2-like markers in RAW264.7 cells upon stimulation with IL-4 and IL-13. Statistical significance was determined by ANOVA.

expression and phosphorylation were unaffected by SMEPPI (Fig. 3A). Nuclear localization of p65 was significantly decreased by SMEPPI, as determined by immunofluorescence staining and quantification (Fig. 3B). Notably, SMEPPI reduced the expression of Akt Ser/Thr kinase, a p65 kinase, but it did not affect the expression and activation of other p65 kinases, including p38, extracellular signal-regulated kinase (ERK), and IκB kinase (IKK) β (Fig. 3C). SMEPPI also decreased the expression and phosphorylation levels of p65 and reduced Akt expression in RAW264.7 cells (Fig. 3D). SMEPPI also suppressed the nuclear localization of p65 in RAW264.7 cells (Fig. 3E), indicating the potential of SMEPPI to inhibit the expression and activation of p65.

2.4. Increased NF-κB p65 proteasomal degradation by SMEPPI

As expected, the decrease in endogenous p65 expression and activation by SMEPPI led to a decrease in the promoter activity of the IL-6 gene, which is a target of p65 in RAW264.7 macrophages stimulated by LPS (Fig. 4A). We hence overexpressed p65 in HEK293T cells to evaluate the effect of SMEPPI on the transcriptional activity of p65. The NF-κB promoter activity was markedly increased by p65 overexpression, which could be decreased by SMEPPI (Fig. 4B). Interestingly, SMEPPI decreased the expression levels of overexpressed p65 in a concentration-dependent manner, and this was blocked by the proteasome inhibitor MG132 (Fig. 4C and D), suggesting that SMEPPI promotes p65 protein degradation. Further RNA sequencing (RNA-seq) analysis demonstrated that SMEPPI increased the expression of ubiquitin-proteasomal degradation-related molecules (Fig. 4E). Quantitative PCR (qPCR) verified that SMEPPI significantly increased the expression of tripartite motif containing 3 (Trim3), ubiquitin-conjugating enzyme 2 s (Ube2S), ubiquitin-protein ligase E3 component n-recognin 7 (Ubr7), and Deltex4 (Dtx4) in M1 macrophages (Fig. 4F), which is in keeping with the promotion of proteasome-mediated p65 degradation by SMEPPI.

2.5. Enhanced phagocytic activity of macrophages by SMEPPI

In addition, the RNA-seq analysis showed that SMEPPI increased the expression of lectin family and membrane and lysosome-related genes involved in macrophage phagocytosis (Fig. 5A). We further validated that SMEPPI substantially increased the expression of phagocytosis-related genes such as *Lgals3*, *Clec7a*, *Lipa*, *Laptm4b*, *Cd68*, and *Cd33* in M1 macrophages (Fig. 5B), suggesting that SMEPPI can enhance the phagocytic activity of macrophages. Flow cytometry and immunofluorescence staining using fluorescence-labeled zymosan bioparticle further confirmed that SMEPPI significantly increased the phagocytic activity of M1 macrophages (Fig. 5C and D). SMEPPI also enhanced the phagocytic activity of RAW264.7 macrophages in a concentration-dependent manner (Fig. 5E), indicating the potential of SMEPPI to promote macrophage phagocytosis.

2.6. Anti-inflammatory and anti-septic activities of SMEPPI in vivo

Having shown that SMEPPI inhibited the production of pro-inflammatory cytokines in M1 macrophages *in vitro*, we examined its anti-inflammatory and protective effects against lung injury *in vivo*. Mice were injected intraperitoneally with different concentrations of SMEPPI for seven days and their lungs were then analyzed after intratracheal instillation of LPS. Intratracheal LPS instillation caused severe lung inflammation and airway epithelial cell injury, which was attenuated by pre-treatment with SMEPPI (Fig. 6A). Additionally, LPS increased the infiltration of $CD11b^{+}$ as well as $F4/80^{+}$ macrophages into the injured lung tissue, whereas SMEPPI decreased the infiltration of macrophages into the lung in a dose-dependent manner. Interestingly, the expression

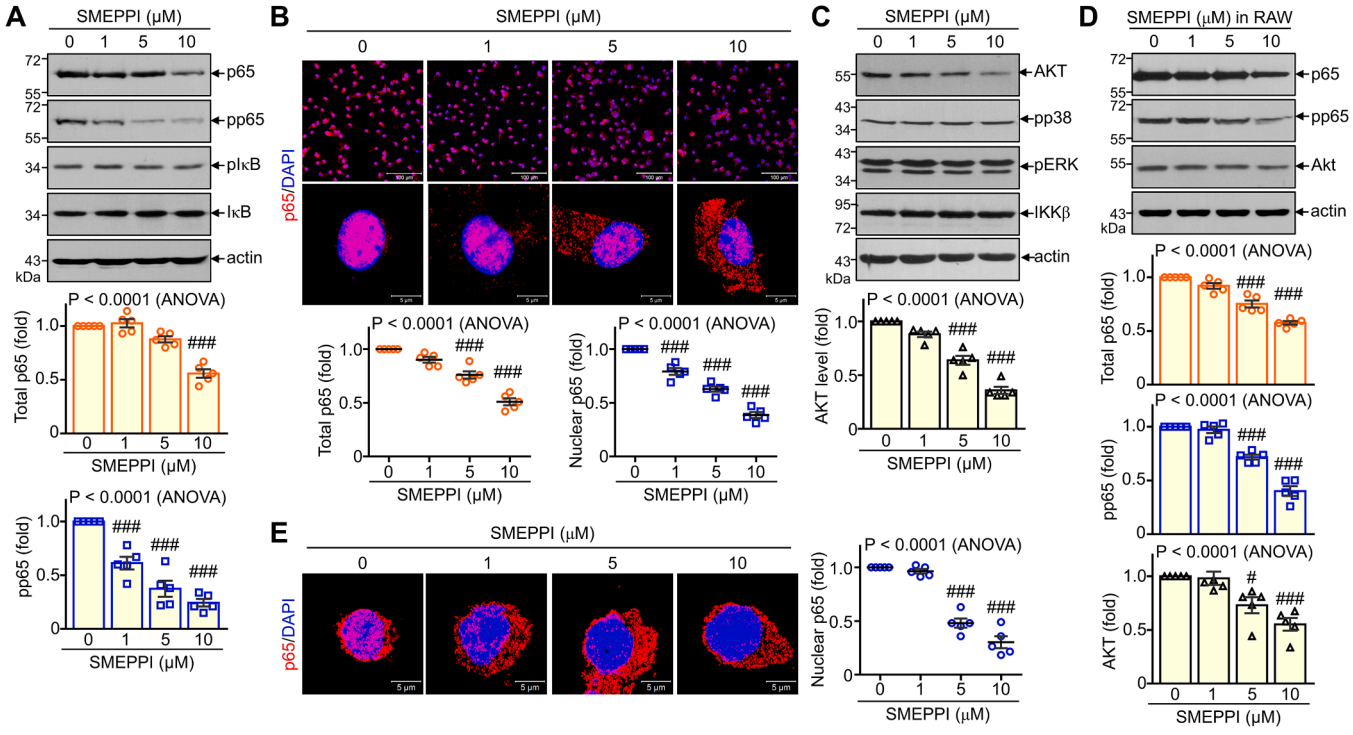

Fig. 3. Suppression of p65 expression and phosphorylation by SMEPPI. (**A–C**) Primary M1 macrophages were incubated with different concentrations of SMEPPI for 24 h, followed by immunoblot analysis and immunofluorescence staining. Protein expression levels were analyzed with specific antibodies and quantified using ImageJ software (**A**). The cells were fixed and immunostained with p65 antibody, followed by fluorescence microscopy; total and nuclear levels of p65 were quantitatively determined (**B**). Cellular levels of kinases were evaluated in M1 macrophages and quantified (**C**). (**D**, **E**) RAW264.7 macrophages were incubated with SMEPPI and subjected to immunoblot analysis of p65, pp65, and Akt. Relative protein band intensities were determined by comparison with the vehicle control (**D**). The cells were fixed and stained with a p65 antibody, and cellular p65 expression was observed and quantified using a fluorescence microscope (**E**). The data are shown as the mean ± SEM of five independent experiments. #P < 0.05; ###P < 0.0005 by ANOVA with Tukey's HSD post-hoc test.

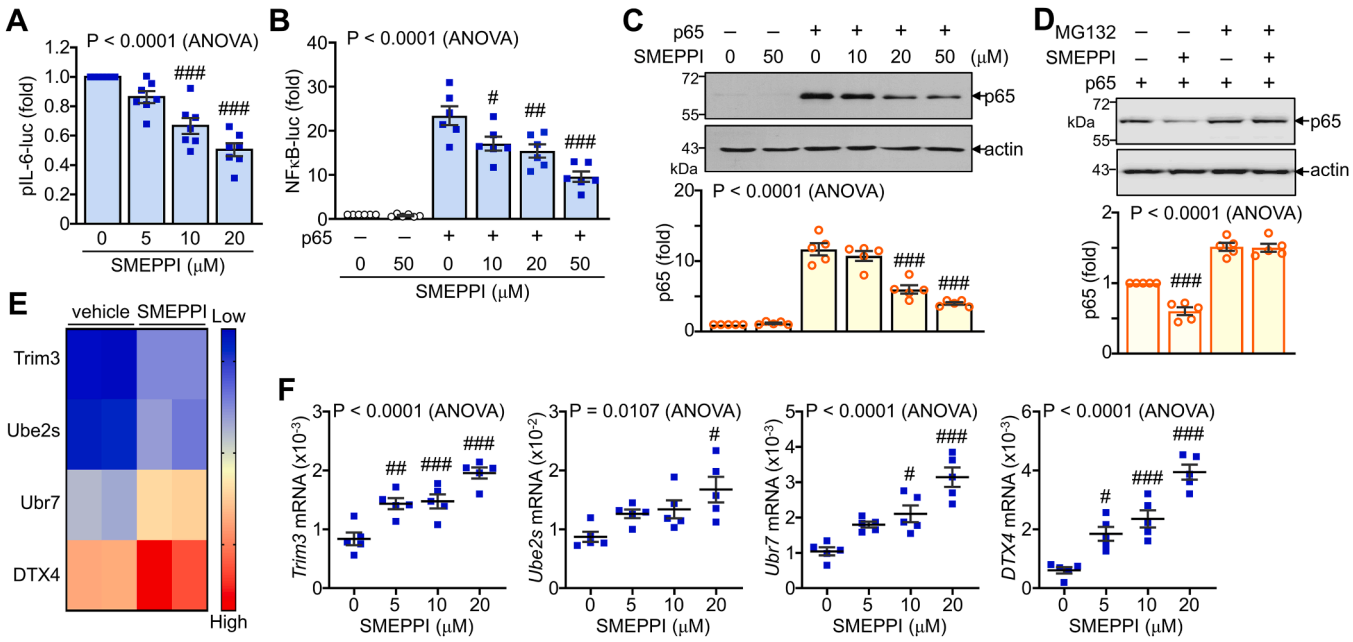

Fig. 4. SMEPPI-induced p65 degradation through activation of the proteasomal degradation system. (**A**) IL-6 promoter activity was evaluated in the presence of SMEPPI in RAW264.7 macrophages. (**B**) NF-κB activity by p65 overexpression was determined in the presence of SMEPPI. (**C**) Effects of SMEPPI on p65 protein levels overexpressed in HEK293T cells. (**D**) HEK293T cells were transfected with p65 and incubated with SMEPPI in the presence or absence of MG132 (10 μM), followed by immunoblotting analysis. (**E**) M1 macrophages were incubated with SMEPPI (10 μM) for 24 h and subjected to RNA-seq analysis. The heatmap of genes involved in the proteasome system with or without SMEPPI is presented. (**F**) Quantitative analysis of proteasomal genes in primary M1 macrophages after treatment with different concentrations of SMEPPI. The data are the mean ± SEM of five independent experiments. #P < 0.05; ##P < 0.005; ###P < 0.0005 by ANOVA with Tukey's HSD post-hoc test.

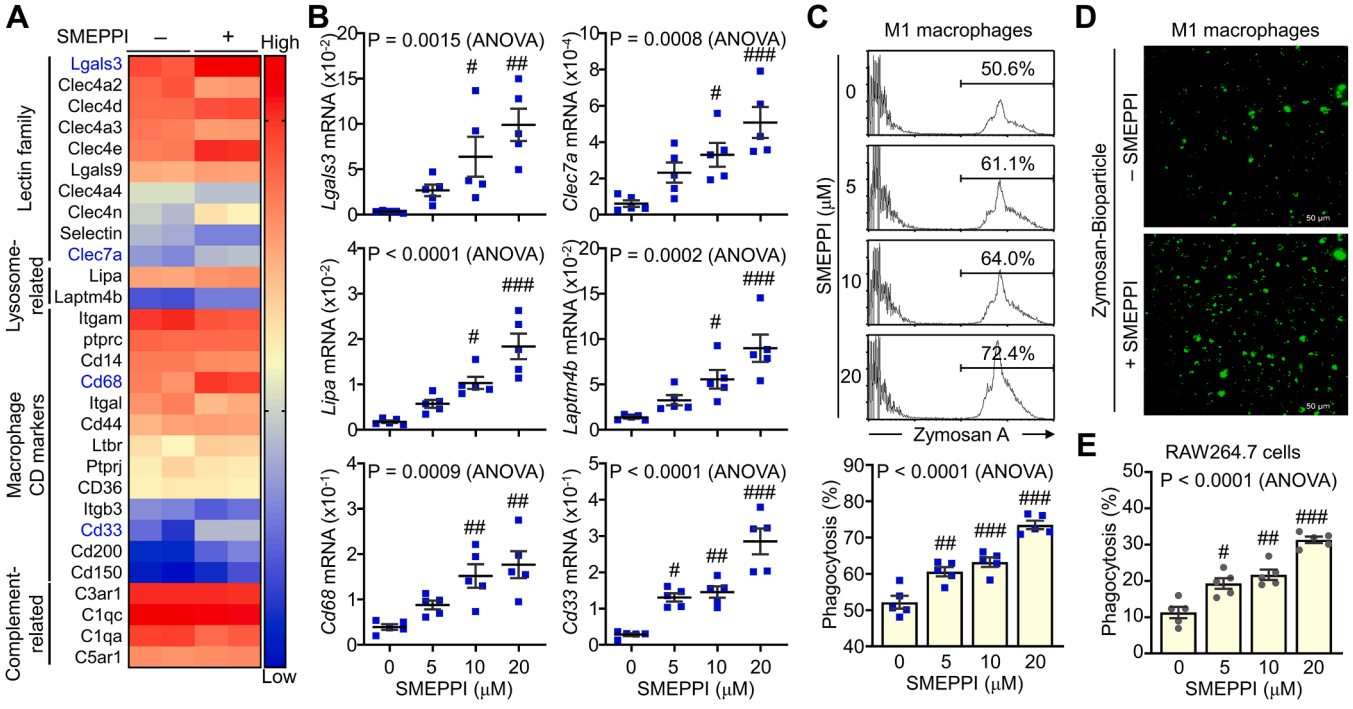

Fig. 5. Increased expression of macrophage surface markers and enhanced phagocytosis by SMEPPI. (**A–D**) Primary M1 macrophages were treated with SMEPPI (10 μM) and subjected to RNA extraction. The heatmap of macrophage-specific markers from the RNA-seq analysis is shown (**A**). Quantitative analysis of macrophage-specific markers using qPCR (**B**). Quantitative phagocytosis assays of M1 macrophages after treatment with SMEPPI (**C**). Fluorescence imaging of zymosan bioparticle was captured in M1 macrophages treated with SMEPPI (**D**). (**E**) RAW264.7 macrophages were treated with SMEPPI, followed by a zymosan-based phagocytosis assay. The data are expressed as the mean ± SEM. #P < 0.05; ##P < 0.005; ###P < 0.0005 by ANOVA with Tukey's HSD post-hoc test.

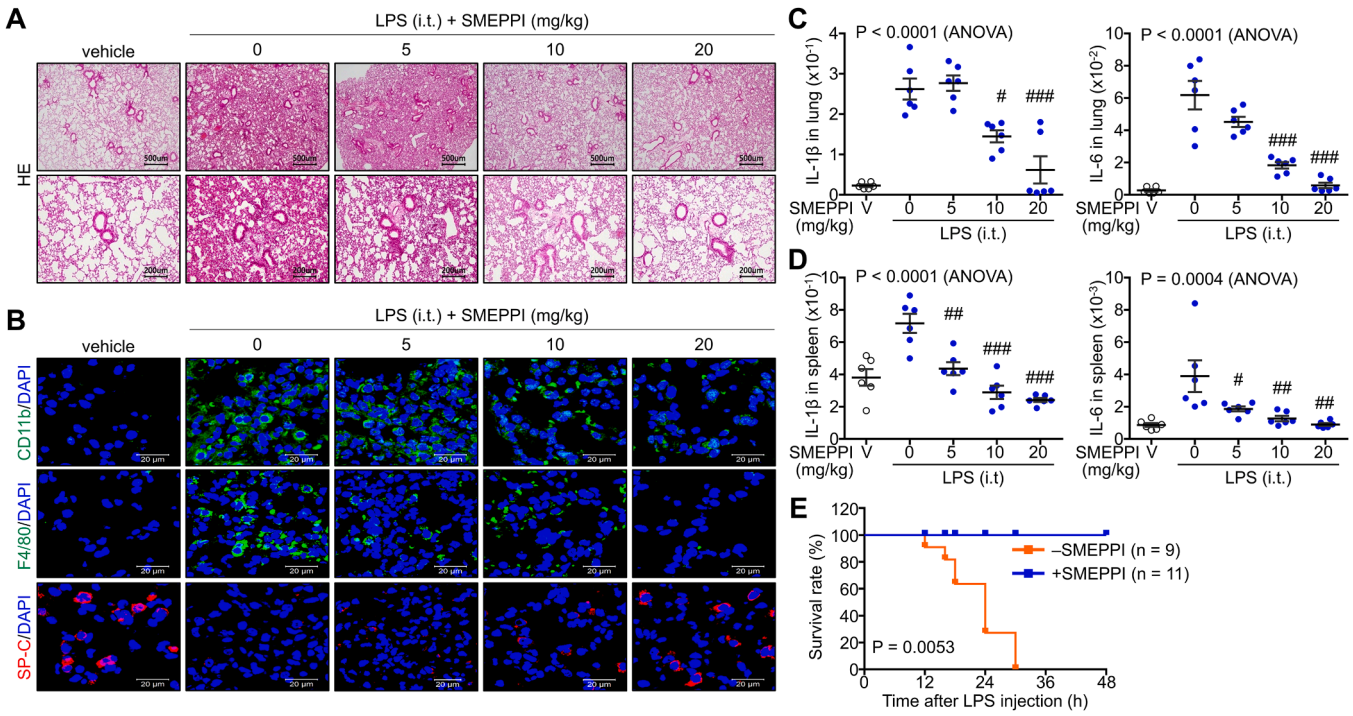

Fig. 6. Suppression of acute lung injury and mortality by SMEPPI. C57BL/6 mice were intraperitoneally injected with either vehicle (n = 6) or different concentrations of SMEPPI (n = 6 per group) for 5 days and exposed to LPS (10 mg/kg) via intratracheal instillation. (**A**) After overnight LPS instillation, lung tissues were sectioned and subjected to HE staining. (**B**) Immunohistochemistry of lung tissues using antibodies against CD11b, F4/80, and SP-C. (**C**) Lung tissues were harvested for RNA extractions, and the relative expression levels of inflammatory cytokines were determined using qPCR. (**D**) Splenic cells were harvested and subjected to RT and qPCR analysis. (**E**) The effects of SMEPPI on the mortality rate of mice upon LPS-induced acute lung injury. The mice were injected with vehicle (n = 9) or SMEPP (n = 11) for 5 days and then exposed to LPS. The mice were monitored for 3 days, and their survival rate was determined. The data are expressed as the mean ± SEM. #P < 0.05; ##P < 0.005; ###P < 0.0005 by ANOVA with Tukey's HSD post-hoc test.

of surfactant protein-C (SP-C), a lung epithelial cell marker, was significantly decreased by LPS, but its expression was increased in a dose-dependent manner in the mouse lung tissue injected with SMEPPI (Fig. 6B), suggesting a protective role of SMEPPI against lung injury. As expected, the expression of pro-inflammatory cytokines was drastically decreased by SMEPPI in both the lung tissue and spleen (Fig. 6C and D). Furthermore, SMEPPI significantly increased the survival rate of mice with LPS-induced septic shock (Fig. 6E), indicating the potent anti-inflammatory and anti-septic effects of SMEPPI against LPS-induced injury *in vivo*.

3. Discussion

In this study, we found that the indenone derivative SMEPPI, specifically suppressed IL-6, IL-1β, and TNF-α expression in M1 macrophages. This was mediated by a decrease in p65 phosphorylation through a decrease in Akt expression, and a concomitant decrease in p65 expression through an increase in the expression of proteasome-related genes. We also found that SMEPPI promoted macrophage phagocytosis by inducing the expression of phagocytic molecules. Furthermore, SMEPPI ameliorated actual LPS-induced lung injury and increased the survival rate of mice against septic shock.

Indanone/indenone derivatives exert diverse biological activities, including neuroprotective, anti-inflammatory, and anti-diabetic effects [21–27]. The indenone derivative KR-62980 exhibits anti-allergic activity by inhibiting CD4 T cell proliferation and by suppressing Th2 cell cytokines associated with allergic reactions. It also exhibits anti-adipogenic activity by inhibiting lipase activity and by increasing PPARγ suppression [17–20]. However, the effects of indanone/indenone derivatives on macrophage activity and their impact on macrophage-mediated inflammatory diseases have not been investigated to date. We therefore assessed whether the indenone derivative SMEPPI could exhibit an anti-inflammatory effect through direct regulation of M1 macrophages and whether it could protect from lung injury and septic shock upon LPS injection *in vivo*. Our findings reiterate the anti-inflammatory effect of the indenone structure and its potential to modulate inflammatory diseases. Our results also highlight that SMEPPI may be beneficial in preventing or ameliorating inflammatory diseases, such as acute lung injury and sepsis.

Our RNA-seq analysis demonstrated that SMEPPI increased the expression of several ubiquitin-conjugating enzymes and ubiquitin ligases involved in the ubiquitin-proteasomal degradation pathway [28]. The levels of Trim3, Ube2s, Ubr7, and Dtx4, which play roles in ubiquitin-mediated protein degradation [29–32], were increased by SMEPPI in a dose-dependent manner. Because p65 protein stability is regulated by the ubiquitin-mediated proteolytic and lysosomal degradation pathways [33–35], the ubiquitin-related genes increased by SMEPPI may directly decrease p65 protein stability. For example, Trim family E3 ligases act as critical regulators of the NF-κB pathway and are involved in the development of NF-κB-mediated inflammatory diseases [31]. However, further studies are needed to clarify whether and how p65 is directly regulated by Trim3, Ube2s, Ubr7, and Dtx4.

In addition to the proteasome-related genes, SMEPPI also induced the expression of macrophage phagocytic genes, which include lectin family members, lysosomal genes, and macrophage surface markers, such as Lgals3, Clec7a, Cd68, Cd33, Lipa, and Laptm4b [36–41]. Galectin-3, encoded by the *Lgals3* gene is known to promote phagocytosis of apoptotic cells, and its deficiency is consistent with reduced efferocytosis observed in human asthma [36,42]. Phagocytic C-type lectins (Clec family) directly recognize pathogens on the surface of microbes and mediate phagocytosis [37]. Increased expression of these membrane proteins and lysosomal proteins in macrophages may increase their ability to recognize and bind to target cells, resulting in efficient phagocytosis and degradation. Therefore, increased expression

of membrane surface markers and lysosomal proteins in M1 macrophages by SMEPPI promotes M1 macrophage phagocytosis. Although the expression of phagocytic genes was increased by SMEPPI, it is still unclear how SMEPPI induces the transcription of these gene and how these phagocytosis genes are involved in the promotion of phagocytosis at the molecular level.

4. Materials and methods

4.1. Materials

The cytokines M-CSF, IL-4, and IL-13 were purchased from R&D Systems (Minneapolis, MN, USA). LPS, carboxyfluorescein diacetate succinimidyl ester (CFSE), and MG132 were purchased from Sigma-Aldrich (St. Louis, MO, USA). The synthesized SMEPPI had 98 % purity and was used for all the *in vitro* and *in vivo* experiments. Antibodies against Akt, IκB, IKKβ, pIκB, pp65, p65, pp38, pERK, and actin were obtained from Cell Signaling Technology (Danvers, MA, USA), Santa Cruz Biotechnology Inc. (Santa Cruz, CA, USA), or Bioss (Woburn, MA, USA).

4.2. Cell culture and viability assay

BMDMs were isolated from male C57BL/6 mice by flushing the femurs and tibia with DMEM supplemented with 10 % FBS. The BMDMs were induced to proliferate by treatment with M-CSF (10 ng/mL), which was replaced with fresh M-CSF medium every other day for 7 days. The cells were treated with IL-4 (10 ng/mL) and IL-13 (10 ng/mL) for M2 polarization or LPS (100 ng/mL) for M1 polarization for 24 h. RAW264.7 macrophages (TIB-71, ATCC, Manassas, VA, USA) were maintained in DMEM and treated with SMEPPI. For the cell viability assay, BMDMs or activated macrophages were treated with SMEPPI for 24 h, followed by incubation with EZ-Cytox reagent for 30 min according to the manufacturer's instructions (EZ-Cytox Cell Viability Assay Kit, DoGenBio, Seoul, Korea). The optical density was determined using a microplate reader (Molecular Devices, Sunnyvale, CA, USA) at the Ewha Fluorescence Imaging Core Center.

4.3. Cell proliferation analysis

BMDMs were stained with CFSE (5 μM) for 15 min and incubated with SMEPPI (100 μM) in the presence of M-CSF (10 ng/mL) for 4 days with replacement of the medium every other day. The cells were harvested on days 0, 1, 2, 3, and 4 and then subjected to flow cytometric analysis using a BD FACS Caliber (BD Biosciences, San Jose, CA, USA). Proliferating cells were quantitatively analyzed using CellQuest software (BD Biosciences).

4.4. RNA-seq and qPCR analysis

M1 macrophages derived from BMDMs were incubated with SMEPPI (10 μM) for 24 h and harvested for RNA extraction using TRIzol reagent (Thermo Fischer Scientific, Carlsbad, CA, USA). The RNA-seq assay was performed by Ebiogen Inc. (Seoul, Korea). Total RNA was prepared from M1 macrophages or RAW264.7 cells treated with different concentrations of SMEPPI and subjected to reverse transcription and qPCR analysis using Thunderbird SYBR qPCR Mix (Toyobo, Osaka, Japan) and a Step-One-Plus real-time PCR system (Applied Biosystems, Carlsbad, CA, USA). The relative transcript levels of the genes were calculated after normalization with the Ct values of the β-actin gene. The specific primer sets used were as follows: IL-1β, 5′-caaccaacaagtgatattctccat-3′, 5′-gatccacactctccagctgca-3′; IL-6, 5′-accacttcacaagtcggagg-3′, 5′-tccaggtagctatggtactcc-3′; TNFα, 5′-cagttctatggcccagaccctca-3′, 5′-acaaccatcggctggcaccac-3′; Trim3, 5′-gctctggtcagcgacttggag-3′, 5′-ccaggttgagcaccgatctc-3′; Ube2s, 5′-tgctgaccatcaagtgcctg-3′, 5′-ctacagtcgcctcagtgctc-3′; Ubr7, 5′-gccacagtccagctgcagac-3′, 5′-cttctctcttaacaaccgtgcc-3′; Dtx4, 5′-catctactgcctggtggctatg-3′, 5′-ttcggatgctctggtccctg-3′; Lgals3, 5′-actgacggtgccctatgacc-3′, 5′-gtaggtgagcatcgttgacc-3′; Clec7a, 5′-cccagctaggtgctcatctactg-3′, 5′-gtgcagtaagctttcctgggg-3′; Lipa, 5′-tggtgaggaacactcggtcc-3′, 5′-ccagcatccgccaggaggaag-3′; Laptm4b, 5′-acatgctgcctggatcatccc-3′, 5′-accaggacatcggaggagttc-3′; Cd68, 5′-tcagggtggaagaaaggcttggg-3′, 5′-ttccaccgccatgtagtcc-3′; Cd33, 5′-tcaagaggcaggaagcgatcac-3′, 5′-ggaagccatagaggacacagg-3′; β-actin, 5′-caccctgtgctgctcaccgag-3′, 5′-accgctcgttgccaatagtga-3′.

4.5. Immunofluorescence staining

For immunofluorescence staining, primary M1 macrophages and RAW264.7 cells were plated on poly-L-lysine-coated glass coverslips (Marienfeld, Lauda-Königshofen, Germany) and incubated with different concentrations of SMEPPI for 24 h. The cells were then fixed and stained with antibodies against NF-κB p65, followed by DAPI staining (1 μg/mL, Sigma-Aldrich) and observation using a fluorescence microscope (Axio Observer 7, Carl Zeiss, Jena, Germany) at the Ewha Drug Development Research Core Center. Total and subcellular fluorescence intensities were quantified using ImageJ software (NIH, Bethesda, MD, USA).

4.6. Immunoblot analysis

The cells were treated with SMEPPI and subjected to protein extraction using RIPA lysis buffer. Protein lysates were resolved by SDS-PAGE, transferred to nitrocellulose membranes, and incubated with primary and secondary antibodies. Protein signals were visualized after incubation with electrochemical luminescence detection reagent using Amersham ImageQuant 800 (Cytiva, Marlborough, MA, USA) and quantified using ImageJ software.

4.7. Reporter gene assay

RAW264.7 cells were transfected with the reporter genes pIL-6-luc and RSVβ and then incubated with SMEPPI for 24 h. HEK-293T cells were transfected with the p65 expression vector and reporter genes NF-κB-luc and RSVβ and incubated with SMEPPI for an additional 24 h. The reporter gene RSVβ was transfected as a positive control for transfection efficiency. The cells were harvested and subjected to luciferase and β-galactosidase assays (Promega, Madison, WI, USA). Luciferase reporter activity was normalized to β-galactosidase activity and expressed as fold-induction.

4.8. Phagocytosis assay

M1 macrophages or RAW264.7 cells were incubated with SMEPPI for 24 h and incubated with pre-labeled zymosan particles (ab234053, Abcam, Cambridge, MA, USA). The cells were fixed and observed using a fluorescence microscope. The cells were subjected to flow cytometric analysis and quantification using CellQuest software.

4.9. LPS-induced acute lung injury model

For *in vivo* efficacy testing of SMEPPI, C57BL6/J mice (male, 8–10 weeks old) were pretreated with different doses of SMEPP (5, 10, and 20 mg/kg) daily for 5 consecutive days via intraperitoneal injection. The mice were then exposed to LPS (10 mg/kg, intratracheal instillation), and the survival rate was monitored for 3 days. All animal experiments were conducted according to international animal welfare guidelines, and all procedures were approved by the Institutional Animal Care and Use Committee of Ewha Womans University (IACUC 19–010 and 21–072).

4.10. Histological analysis

After overnight LPS treatment, the mice were sacrificed, and lung tissue samples were harvested, fixed in 10 % formaldehyde solution for 24 h, and embedded in paraffin. Lung tissues were sectioned at 4-μm thickness and subjected to hematoxylin and eosin (HE, Sigma-Aldrich) staining or immunohistochemistry. HE-stained lung tissues were observed and photographed under an upright microscope (Nikon Eclipse Ci, Nikon, Tokyo, Japan). For immunohistochemistry, lung tissues were incubated with antibodies against macrophage markers CD11b and F4/80 and lung epithelial cell marker SP-C, followed by incubation with fluorescence-conjugated antibodies and DAPI solution (1 μg/mL, Sigma-Aldrich).

4.11. Statistical analysis

All experiments were performed at least five times, and all data are expressed as the mean ± standard error of the mean (SEM). All statistical analyses were performed using GraphPad Prism version 10.0 software (GraphPad Inc., San Diego, CA, USA). The statistical significance of the mean differences was analyzed using a one-way analysis of variance (ANOVA) with Tukey's HSD post-hoc test. P values < 0.05 were considered statistically significant.

Funding

This work was supported by grants from the National Research Foundation [NRF-2018R1A5A2025286 and 2020R1A2C2004679 for ESH and RS-2023–00221182 for JHH] funded by the Ministry of Science and ICT of Korea.

CRediT authorship contribution statement

Jin-Hee Ahn: Resources, Methodology, Investigation. **Myung Ae Bae:** Resources, Project administration, Conceptualization. **Eun Sook Hwang:** Writing – review & editing, Writing – original draft, Supervision, Project administration, Funding acquisition. **Jeong-Ho Hong:** Writing – review & editing, Investigation, Conceptualization. **Soheun Lee:** Methodology, Data curation. **Mi Gyeong Jeong:** Methodology, Investigation. **Jio Kang:** Methodology. **Jihae Lim:** Methodology. **Ji Hyun Oh:** Validation, Methodology, Formal analysis, Data curation.

Declaration of Generative AI and AI-assisted technologies in the writing process

No declaration of generative AI and AI-assisted technologies

Declaration of Competing Interest

The authors declare no competing financial interests.

Acknowledgments

None.

Author contributions

JHO and MGJ performed most of the experiments and SL, JL, and JK conducted the animal experiments. MAB and JHA designed, synthesized, and purified SMEPPI. JHH and ESH devised the experimental strategies and discussed the results. ESH prepared the manuscript for publication.

Data availability

Data will be made available on request.

References

[1] M.E. Kotas, R. Medzhitov, Homeostasis, inflammation, and disease susceptibility, Cell 160 (2015) 816–827, https://doi.org/10.1016/j.cell.2015.02.010.
[2] M.L. Meizlish, R.A. Franklin, X. Zhou, R. Medzhitov, Tissue homeostasis and inflammation, Annu Rev. Immunol. 39 (2021) 557–581, https://doi.org/10.1146/annurev-immunol-061020-053734.
[3] C. Bleriot, S. Chakarov, F. Ginhoux, Determinants of resident tissue macrophage identity and function, Immunity 52 (2020) 957–970, https://doi.org/10.1016/j.immuni.2020.05.014.
[4] P. Rodriguez-Morales, R.A. Franklin, Macrophage phenotypes and functions: resolving inflammation and restoring homeostasis, Trends Immunol. 44 (2023) 986–998, https://doi.org/10.1016/j.it.2023.10.004.
[5] C. Atri, F.Z. Guerfali, D. Laouini, Role of human macrophage polarization in inflammation during infectious diseases, Int J. Mol. Sci. 19 (2018), https://doi.org/10.3390/ijms19061801.
[6] M. Luo, F. Zhao, H. Cheng, M. Su, Y. Wang, Macrophage polarization: an important role in inflammatory diseases, Front Immunol. 15 (2024) 1352946, https://doi.org/10.3389/fimmu.2024.1352946.
[7] L.S. Bisgaard, C.K. Mogensen, A. Rosendahl, H. Cucak, L.B. Nielsen, S. E. Rasmussen, T.X. Pedersen, Bone marrow-derived and peritoneal macrophages have different inflammatory response to oxLDL and M1/M2 marker expression - implications for atherosclerosis research, Sci. Rep. 6 (2016) 35234, https://doi.org/10.1038/srep35234.
[8] T.A. Wynn, A. Chawla, J.W. Pollard, Macrophage biology in development, homeostasis and disease, Nature 496 (2013) 445–455, https://doi.org/10.1038/nature12034.
[9] E. Mass, F. Nimmerjahn, K. Kierdorf, A. Schlitzer, Tissue-specific macrophages: how they develop and choreograph tissue biology, Nat. Rev. Immunol. 23 (2023) 563–579, https://doi.org/10.1038/s41577-023-00848-y.
[10] S. Chen, A. Saeed, Q. Liu, Q. Jiang, H. Xu, G.G. Xiao, L. Rao, Y. Duo, Macrophages in immunoregulation and therapeutics, Signal Transduct. Target Ther. 8 (2023) 207, https://doi.org/10.1038/s41392-023-01452-1.
[11] J.H. Ahn, M.S. Shin, S.H. Jung, S.K. Kang, K.R. Kim, S.D. Rhee, W.H. Jung, S. D. Yang, S.J. Kim, J.R. Woo, J.H. Lee, H.G. Cheon, S.S. Kim, Indenone derivatives: a novel template for peroxisome proliferator-activated receptor gamma (PPARgamma) agonists, J. Med Chem. 49 (2006) 4781–4784, https://doi.org/10.1021/jm060389m.
[12] G. Zou, T. Li, W. Yang, B. Sun, Y. Chen, B. Wang, Y. Ou, H. Yu, Z. She, Antioxidative indenone and benzophenone derivatives from the mangrove-derived fungus cytospora heveae NSHSJ-2, Mar. Drugs 21 (2023), https://doi.org/10.3390/md21030181.
[13] S. Raza, S.P. Srivastava, D.S. Srivastava, A.K. Srivastava, W. Haq, S.B. Katti, Thiazolidin-4-one and thiazinan-4-one derivatives analogous to rosiglitazone as potential antihyperglycemic and antidyslipidemic agents, Eur. J. Med Chem. 63 (2013) 611–620, https://doi.org/10.1016/j.ejmech.2013.01.054.
[14] X. Xiong, Y. Ye, L. Fu, B. Dai, J. Liu, J. Jia, J. Tang, L. Li, L. Wang, J. Shen, C. Mei, Antitumor activity of a novel series of alpha-aryloxy-alpha-methylhydrocinnamic acid derivatives as PPAR gamma agonists against a panel of human cancer cell lines, Invest N. Drugs 27 (2009) 223–232, https://doi.org/10.1007/s10637-008-9161-0.
[15] J. Kim, D.C. Han, J.M. Kim, S.Y. Lee, S.J. Kim, J.R. Woo, J.W. Lee, S.K. Jung, K. S. Yoon, H.G. Cheon, S.S. Kim, S.H. Hong, B.M. Kwon, PPAR gamma partial agonist, KR-62776, inhibits adipocyte differentiation via activation of ERK, Cell Mol. Life Sci. 66 (2009) 1766–1781, https://doi.org/10.1007/s00018-009-9169-4.
[16] J. Priyanga, B. Sharan Kumar, R. Mahalakshmi, K. Nirekshana, P. Vinoth, V. Sridharan, D. Bhakta-Guha, G. Guha, A novel indenone derivative selectively induces senescence in MDA-MB-231 (breast adenocarcinoma) cells, Chem. Biol. Inter. 331 (2020) 109250, https://doi.org/10.1016/j.cbi.2020.109250.
[17] K.R. Kim, J.H. Lee, S.J. Kim, S.D. Rhee, W.H. Jung, S.D. Yang, S.S. Kim, J.H. Ahn, H.G. Cheon, KR-62980: a novel peroxisome proliferator-activated receptor gamma agonist with weak adipogenic effects, Biochem Pharm. 72 (2006) 446–454, https://doi.org/10.1016/j.bcp.2006.05.005.
[18] H.S. Chun, S.H. Shin, S. Ahn, D.S. Shin, S.S. Choi, J.H. Ahn, M.A. Bae, KR-62980 suppresses lipid metabolism through inhibition of cytosolic NADP isocitrate dehydrogenase in zebrafish, Zebrafish 11 (2014) 122–128, https://doi.org/10.1089/zeb.2013.0919.
[19] H. Jung, M.S. Lee, E.J. Jang, J.H. Ahn, N.S. Kang, S.E. Yoo, M.A. Bae, J.H. Hong, E. S. Hwang, Augmentation of PPARgamma-TAZ interaction contributes to the anti-adipogenic activity of KR-62980, Biochem Pharm. 78 (2009) 1323–1329, https://doi.org/10.1016/j.bcp.2009.07.001.
[20] H.Y. Won, H.J. Min, J.H. Ahn, S.E. Yoo, M.A. Bae, J.H. Hong, E.S. Hwang, Anti-allergic function and regulatory mechanisms of KR-62980 in allergen-induced airway inflammation, Biochem Pharm. 79 (2010) 888–896, https://doi.org/10.1016/j.bcp.2009.10.023.
[21] K.Y. Kim, H.S. Cho, S.H. Lee, J.H. Ahn, H.G. Cheon, Neuroprotective effects of KR-62980, a new PPARgamma agonist, against chemical ischemia-reperfusion in SK-N-SH cells, Brain Res 1372 (2011) 103–114, https://doi.org/10.1016/j.brainres.2010.11.062.
[22] G.V. Karunakar, C.E. Raju, G. Sreenivasulu, P.B. Kumar, V. Kadiyala, B. Sridhar, Cationic gold-catalyzed intramolecular cyclization of substituted 1,5-diynes to access indenone derivatives, Chem. Asian J. 17 (2022) e202101408, https://doi.org/10.1002/asia.202101408.
[23] R. Bansal, R. Singh, T.S. Dutta, Z.A. Dar, A. Bajpai, Indanone: a promising scaffold for new drug discovery against neurodegenerative disorders, Drug Discov. Today 29 (2024) 104063, https://doi.org/10.1016/j.drudis.2024.104063.

[24] A. Rauf, U. Rashid, Z.A. Shah, A.A. Khalil, M. Shah, T. Tufail, G. Rehman, A. Rahman, S. Naz, A. Alsahammari, M. Alharbi, A. Al-Shahrani, D. Formanowicz, Anti-inflammatory and anti-diabetic properties of indanone derivative isolated from Fernandoa adenophylla in vitro and in silico studies, Sci. Rep. 14 (2024) 9624, https://doi.org/10.1038/s41598-024-59703-2.
[25] M.A. Ernst-Russell, C.L. Chai, J.H. Wardlaw, J.A. Elix, Euplectin and coneuplectin, new naphthopyrones from the lichen Flavoparmelia euplecta, J. Nat. Prod. 63 (2000) 129–131, https://doi.org/10.1021/np9903245.
[26] H. Kim, I. Yang, S.Y. Ryu, D.H. Won, A.G. Giri, W. Wang, H. Choi, J. Chin, D. Hahn, E. Kim, C. Han, J. Lee, S.J. Nam, W.K. Ho, H. Kang, Acredinones A and B, voltage-dependent potassium channel inhibitors from the sponge-derived fungus Acremonium sp. F9A015, J. Nat. Prod. 78 (2015) 363–367, https://doi.org/10.1021/np5007586.
[27] J.T. Brewster, 2nd, S. Dell'Acqua, D.Q. Thach, J.L. Sessler, Classics in chemical neuroscience: donepezil, ACS Chem. Neurosci. 10 (2019) 155–167, https://doi.org/10.1021/acschemneuro.8b00517.
[28] T. Ravid, M. Hochstrasser, Diversity of degradation signals in the ubiquitin-proteasome system, Nat. Rev. Mol. Cell Biol. 9 (2008) 679–690, https://doi.org/10.1038/nrm2468.
[29] T. Tasaki, L.C. Mulder, A. Iwamatsu, M.J. Lee, I.V. Davydov, A. Varshavsky, M. Muesing, Y.T. Kwon, A family of mammalian E3 ubiquitin ligases that contain the UBR box motif and recognize N-degrons, Mol. Cell Biol. 25 (2005) 7120–7136, https://doi.org/10.1128/MCB.25.16.7120-7136.2005.
[30] J. Cui, Y. Li, L. Zhu, D. Liu, Z. Songyang, H.Y. Wang, R.F. Wang, NLRP4 negatively regulates type I interferon signaling by targeting the kinase TBK1 for degradation via the ubiquitin ligase DTX4, Nat. Immunol. 13 (2012) 387–395, https://doi.org/10.1038/ni.2239.
[31] D. Tomar, R. Singh, TRIM family proteins: emerging class of RING E3 ligases as regulator of NF-kappaB pathway, Biol. Cell 107 (2015) 22–40, https://doi.org/10.1111/boc.201400046.
[32] M.J. Garnett, J. Mansfeld, C. Godwin, T. Matsusaka, J. Wu, P. Russell, J. Pines, A. R. Venkitaraman, UBE2S elongates ubiquitin chains on APC/C substrates to promote mitotic exit, Nat. Cell Biol. 11 (2009) 1363–1369, https://doi.org/10.1038/ncb1983.
[33] A. Ryo, F. Suizu, Y. Yoshida, K. Perrem, Y.C. Liou, G. Wulf, R. Rottapel, S. Yamaoka, K.P. Lu, Regulation of NF-kappaB signaling by Pin1-dependent prolyl isomerization and ubiquitin-mediated proteolysis of p65/RelA, Mol. Cell 12 (2003) 1413–1426, https://doi.org/10.1016/s1097-2765(03)00490-8.
[34] T. Tanaka, M.J. Grusby, T. Kaisho, PDLIM2-mediated termination of transcription factor NF-kappaB activation by intranuclear sequestration and degradation of the p65 subunit, Nat. Immunol. 8 (2007) 584–591, https://doi.org/10.1038/ni1464.
[35] C.P. Chang, Y.C. Su, C.W. Hu, H.Y. Lei, TLR2-dependent selective autophagy regulates NF-kappaB lysosomal degradation in hepatoma-derived M2 macrophage differentiation, Cell Death Differ. 20 (2013) 515–523, https://doi.org/10.1038/cdd.2012.146.
[36] H. Sano, D.K. Hsu, J.R. Apgar, L. Yu, B.B. Sharma, I. Kuwabara, S. Izui, F.T. Liu, Critical role of galectin-3 in phagocytosis by macrophages, J. Clin. Invest 112 (2003) 389–397, https://doi.org/10.1172/JCI17592.
[37] A.M. Kerrigan, G.D. Brown, C-type lectins and phagocytosis, Immunobiology 214 (2009) 562–575, https://doi.org/10.1016/j.imbio.2008.11.003.
[38] J. Zhang, S. Li, F. Liu, K. Yang, Role of CD68 in tumor immunity and prognosis prediction in pan-cancer, Sci. Rep. 12 (2022) 7844, https://doi.org/10.1038/s41598-022-11503-2.
[39] A. Bhattacherjee, E. Rodrigues, J. Jung, M. Luzentales-Simpson, J.R. Enterina, D. Galleguillos, C.D.St Laurent, M. Nakhaei-Nejad, F.F. Fuchsberger, L. Streith, Q. Wang, N. Kawasaki, S. Duan, A. Bains, J.C. Paulson, C. Rademacher, F. Giuliani, S. Sipione, M.S. Macauley, Repression of phagocytosis by human CD33 is not conserved with mouse CD33, Commun. Biol. 2 (2019) 450, https://doi.org/10.1038/s42003-019-0698-6.
[40] M. Viaud, S. Ivanov, N. Vujic, M. Duta-Mare, L.E. Aira, T. Barouillet, E. Garcia, F. Orange, I. Dugail, I. Hainault, C. Stehlik, S. Marchetti, L. Boyer, R. Guinamard, F. Foufelle, A. Bochem, K.G. Hovingh, E.B. Thorp, E.L. Gautier, D. Kratky, P. Dasilva-Jardine, L. Yvan-Charvet, Lysosomal cholesterol hydrolysis couples efferocytosis to anti-inflammatory oxysterol production, Circ. Res 122 (2018) 1369–1384, https://doi.org/10.1161/CIRCRESAHA.117.312333.
[41] Y. Xu, B. Shao, Y. Zhang, The significance of targeting lysosomes in cancer immunotherapy, Front Immunol. 15 (2024) 1308070, https://doi.org/10.3389/fimmu.2024.1308070.
[42] P. Gao, J.L. Simpson, J. Zhang, P.G. Gibson, Galectin-3: its role in asthma and potential as an anti-inflammatory target, Respir. Res 14 (2013) 136, https://doi.org/10.1186/1465-9921-14-136.